43rd Turbomachinery & 30th Pump Users Symposia (Pump & Turbo 2014)
September 23-25, 2014 | Houston, TX | pumpturbo.tamu.edu

OPTIMIZATION OF SWIRL BRAKE DESIGN AND ASSESSMENT OF ITS STABILIZING EFFECT ON COMPRESSOR ROTORDYNAMIC PERFORMANCE

Leonardo Baldassarre
Engineering Executive for Compressors and Auxiliary Systems
General Electric Oil & Gas Company
Florence, Italy

Alberto Guglielmo
Centrifugal Compressor Design Engineer
General Electric Oil & Gas Company
Florence, Italy

Andrea Bernocchi
Senior Engineering Manager for Centrifugal Compressors
General Electric Oil & Gas Company
Florence, Italy

Guido Masi
Centrifugal Compressor Design Engineer
General Electric Oil & Gas Company
Florence, Italy

Michele Fontana
Senior Engineer for Centrifugal CompressorsCompany
Florence, Italy

Leonardo Baldassarre is currently Engineering Executive Manager for Compressors and Auxiliary Systems with GE Oil & Gas, in Florence, Italy. He is responsible for requisition and standardization activities and for the design of new products for compressors, turboexpanders and auxiliary systems.
Dr. Baldassarre began his career with GE in 1997. He worked as Design Engineer, R&D Team Leader, Product Leader for centrifugal and axial compressors and Requisition Manager for centrifugal compressors.
Dr. Baldassarre received a B.S. degree (Mechanical Engineering, 1993) and Ph.D. degree (Mechanical Engineering / Turbomachinery Fluid Dynamics, 1998) from the University of Florence. He authored or coauthored 20+ technical papers, mostly in the area of fluid dynamic design, rotating stall and rotordynamics. He presently holds five patents.

Andrea Bernocchi is an engineering manager at GE Oil&Gas. He joined GE in 1996 as Centrifugal Compressor Design Engineer after an experience in plastic machinery industry. He has 18 years of experience in design development, production and operation of centrifugal compressor. He covered the role of LNG compressor design manager for 6 years with responsibility in design of LNG compressors, testing and supporting plant startup. He's currently leading the requisition team for centrifugal and axial compressor design.
Mr Bernocchi received a B.S. degree in Mechanical Engineering from University of Florence in 1994. He holds 4 patents in compressor field.

Michele Fontana is currently Engineering Manager for Centrifugal Compressor Upstream, Pipeline and Integrally Geared Applications at GE Oil&Gas, in Florence, Italy. He supervises the calculation activities related to centrifugal compressor design and testing, and has specialized in the areas of rotordynamic design and vibration data analysis.
Mr. Fontana graduated in Mechanical Engineering at University of Genova in 2001. He joined GE in 2004 as Centrifugal Compressor Design Engineer, after an experience as Noise and Vibration Specialist in the automotive sector.
He has co-authored six technical papers about rotordynamic analysis and vibration monitoring, and holds two patents in this same field.

Guido Masi is a Lead Design Engineer in Centrifugal Compressor Upstream, Pipeline and Integrally Geared Applications at GE Oil&Gas, in Florence, Italy. His current duties are mainly focused on high pressure compression train design and testing,
Mr. Masi holds a B. S. degree (Mechanical Engineering, 2003) and a Ph.D. degree (Vehicle System Dynamics and Safety Devices, 2008) from University of Firenze. He joined GE Oil&Gas Centrifugal Compressors Requisition team in 2008.

Alberto Guglielmo is a Design Engineer for New Product Introduction group at GE Oil and Gas. He received his M.S. in Mechanical Engineering from the University of Pisa in 2004 and a Ph.D in Mechanical Engineering from the University of Pisa in 2008. He joined GE Oil&Gas in the 2008 working for Requisition team for centrifugal compressor and in 2011 he moved to NPI team. He has been involved into both analytical and experimental structural dynamic and machine design.

ABSTRACT

The rotordynamic stability of high pressure compressors is strongly affected by the aerodynamic effects induced by the gas flow through rotor-stator seals. In particular the tangential velocity (swirl) of the gas flowing through the seals is a main destabilizing factor (Childs, 1993) and therefore needs to be minimized. Swirl brakes are well-known devices to reduce the swirl of the leakage at seal inlet, or preswirl. Their effectiveness is function of several geometrical parameters (swirl brake vane dimensions and shape, clearance gap between rotor and stator, seal diameter) and operating parameters (such as rotating speed, gas pressure, temperature, molecular weight, gas swirl upstream of the seal).

A CFD study was carried out in order to evaluate the impact of each geometrical parameter on swirl brake performance, starting from a baseline and varying it over a possible design range. The purpose was to identify an optimum design that could achieve a strong preswirl reduction over the widest range of compressor applications, sizes and operating conditions.

Swirl brakes developed according to this optimization study were used in a high pressure centrifugal compressor. The full load test performed in 2013 included a direct measurement of the logarithmic decrement, thus providing useful information to validate the outcome of the analysis. A comparison between calculation and test results allowed to verify the effectiveness of swirl brakes, by quantifying the actual preswirl value obtained from the labyrinth seals.

INTRODUCTION

Swirl brakes are widely applied in centrifugal compressors as means of reducing the destabilizing forces originated in rotor-stator non-contacting seals. Their application has negligible impact on aerodynamic efficiency and requires smaller adaptations of compressor design with respect to other devices such as shunt holes (Iwatsubo and Iwasaki, 2002; Moore and Hill, 2000). Swirl brakes consist of a series of radial ribs (or "walls") placed upstream of the seal, whose purpose is to reduce the tangential component (swirl) of the inlet gas flow.

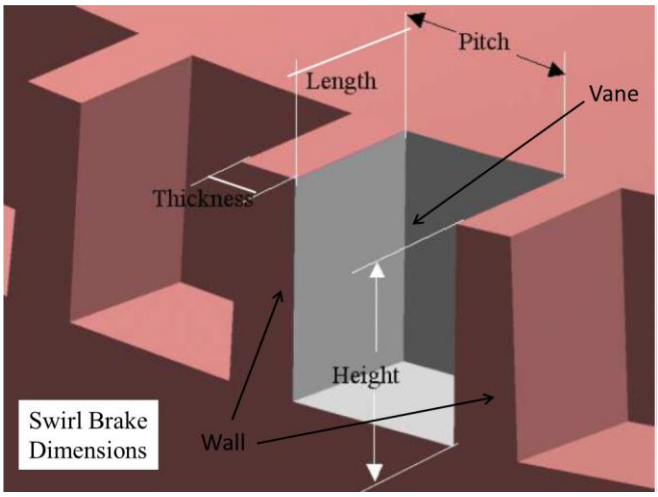

Figure 1. Three-dimensional model of seal with swirl brakes

This is basically achieved by the formation of vortices in the vanes ("vane" is the volume between two consecutive walls, see Fig.1), in which the gas flow is on average straightened along the radial direction and the kinetic energy of the gas is partly dissipated by viscous forces. A seal equipped with swirl brakes is shown in Fig.2, while Fig.3 presents a detail of the swirl brake typical geometry.

The gas velocity distribution inside the swirl brakes, and therefore its effectiveness in reducing the gas swirl, is influenced by a large array of parameters that can be grouped as follows:

- geometry of the seal and of the swirl brakes: diameter D and clearance h of the seal, height H, length A (also called *chord*) and pitch γ of the vane, thickness t and shape of the walls between vanes;
- gas properties: density, viscosity;
- operating conditions: pressure, rotor speed.

Additional parameters can be neglected in a first approximation, such as other physical properties of the gas, the roughness of the surfaces, and the detailed geometry of the flow path upstream and downstream of the swirl brakes.

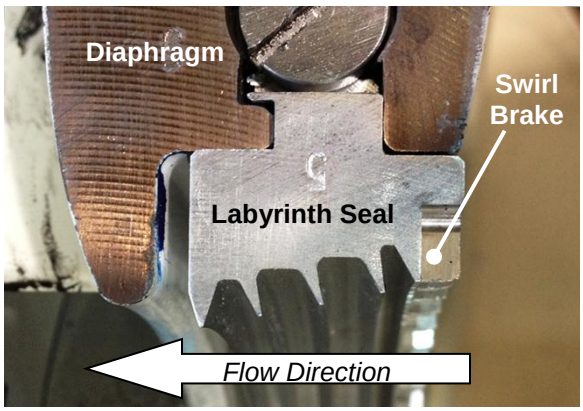

Figure 2. Labyrinth seal equipped with swirl brakes

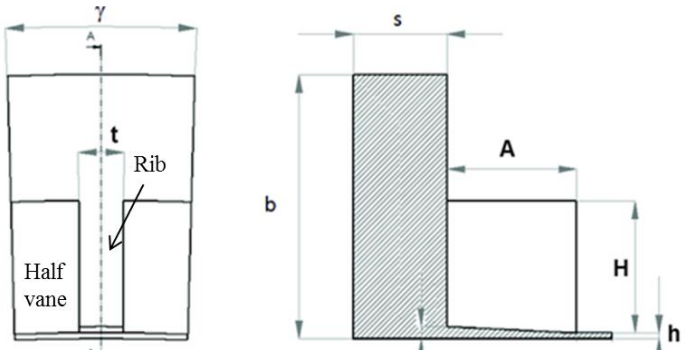

Figure 3. Typical geometry of swirl brakes. Section represents one wall and the two half vanes delimited by it.

An accurate analysis of swirl brake operation shall therefore include quite a large quantity of geometric, thermodynamic and mechanical input parameters, while the most significant output is just a single parameter: the residual tangential component of the velocity of the gas flow downstream of the swirl brakes. This velocity is needed to calculate the destabilizing forces associated to the seals and therefore to estimate the logarithmic decrement of the rotor. This residual tangential velocity is often expressed in terms of swirl ratio (abbreviated as SR; referred also as *preswirl*), that is defined as the ratio between the tangential velocity of the gas and the tangential (tip speed) velocity of the rotor.

The design of a centrifugal compressor equipped with swirl brakes presents two major challenges: how to optimize the geometry of the swirl brake vane to achieve the minimum preswirl, and how to estimate the preswirl magnitude with a sufficient approximation. The present analysis focused on both aspects; the optimization of the geometry based on a Design of Experiments method, starting from a baseline and then analyzing by CFD the effects of variations in each influence parameter. CFD was also used as a first approach for preswirl estimation, with the results later validated through experimental activity. The full load test of a high pressure compressor with swirl brakes on impeller eye labyrinths is taken as benchmark, and the analysis of vibration data allows to evaluate the actual logarithmic decrement in several operating condition. A comparison with calculation results obtained for the same conditions is also used to check and validate the model predictions.

THEORETICAL BACKGROUND

In order to represent the effect of a labyrinth seal on the stability of a rotor, a simple two-dimensional schematic as the one shown in Fig.4a may be considered.

The rotor is surrounded by an annular gas volume, filling the clearance between the seal and the rotor. The gas reaction forces to the displacements of the rotor may be represented with the aid of a stiffness matrix and a damping matrix. The gas real (reaction) forces are modeled as follows:

$$-\begin{pmatrix} F_x \\ F_y \end{pmatrix} = \begin{pmatrix} K_{xx} & k_{xy} \\ k_{yx} & K_{yy} \end{pmatrix} \begin{pmatrix} x \\ y \end{pmatrix} + \begin{pmatrix} C_{xx} & c_{xy} \\ c_{yx} & C_{yy} \end{pmatrix} \begin{pmatrix} \dot{x} \\ \dot{y} \end{pmatrix} \quad (1)$$

where (x,y) are the rotor displacements along the x and y directions, i.e. the components of vector $\boldsymbol{r}$ in Fig.4.

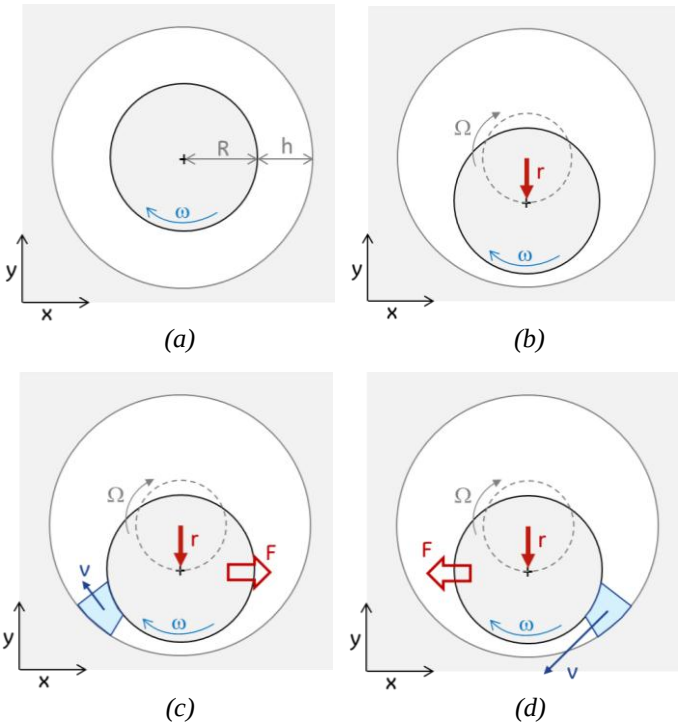

Figure 4. Two-dimensional schematic view of the annular gap between rotor and seal: (a) no offset (zero-amplitude precession orbit); (b) shaft rotating at speed ω and orbiting at speed Ω; (c) gas volume rotating at average velocity lower than Ω: the shaft "pushes forward" the gas; (d) gas volume rotating at average velocity higher than Ω: the shaft is "pushed" by the gas along its orbit.

In the simplified hypothesis of periodic vibration with a circular orbit (x=A$\cos\omega t$, y=A$\sin\omega t$) and assuming that [K] and [C] are skew-symmetric (Muszynska, 2005, p.232), i.e. that

$$K_{xx} = K_{yy} \quad (2)$$

$$k_{xy} = -k_{yx} \quad (3)$$

$$C_{xx} = C_{yy} \quad (4)$$

$$c_{xy} = -c_{yx} \quad (5)$$

the formulation is rewritten as:

$$-F_x = K_{eff}\, x + C_{eff}\, \dot{x} \quad (6)$$

$$-F_y = K_{eff}\, y + C_{eff}\, \dot{y} \quad (7)$$

where the effective stiffness K_{eff} and effective damping C_{eff} are expressed as:

$$K_{eff} = K_{xx} - c_{xy}\omega \quad (8)$$

$$C_{eff} = C_{xx} + \frac{k_{xy}}{\omega} \quad (9)$$

The physical interpretation of the direct stiffness K and the

direct damping *C* coefficients is quite straightforward, at least in the most common situation where both coefficients are positive. A radial displacement of the shaft "pushes away" the gas molecules in front of it, and due to the finite inertia and viscosity of the gas this transmission of motion is neither instantaneous nor frictionless; the shaft therefore experiences a radial stiffness constraining its motion (*K*) and a partial dissipation of its kinetic energy by viscous friction (*C*). According to theory (Muszynska, 2005, Ch.1.5.2), the stiffness term is in phase with the excitation while the viscous damping term lags 90° from it.

The interpretation of the cross-coupled cofficients *k* and *c* is less intuitive, since they define a relation between an exciting force and a displacement that are directed along orthogonal axes. The sketch in Fig.4b aids to the understanding of the phenomenon: it represents a shaft with radius *R* inside a seal with inner radius *R+h*; the shaft rotates around its axis with angular velocity ω and revolves around its vibration axis with angular speed Ω. A forward whirl orbit is assumed, i.e., ω and Ω have the same sign. Due to the radial displacement **r** between the rotor axis and the seal axis, the seal clearance is not uniformly equal to *h* but has a minimum section, where the clearance is *h-r*; the angular position of this minimum section changes during the orbit of the shaft, and therefore with its same precession velocity Ω. The gas volume *V* moves along the annular gap with tangential velocity *v*, and the swirl ratio SR of the gas leakage is defined as

$$SR = v / \omega R \qquad (10)$$

Depending on the value of SR, different situations may occur:

$SR < \Omega/\omega$ The angular velocity (Ω) of the gas volume *V* inside the cavity is lower than the angular speed Ω of the shaft orbit. This means that the shaft has to 'push' the gas tangentially in order to move along its orbit; in doing this, some of the kinetic (vibration) energy of the shaft is transferred to the gas and some is lost through friction losses. This means that the gas in the seal, due to its viscosity and inertia, subtracts energy from the shaft vibration and therefore has a stabilizing effect on the rotor. The cross-coupled coefficients *k* and *c* represent this effect: if the shaft moves along the *x* axis, thus reducing the seal clearance in that direction, it is subject to a force in the *y* direction; this force is caused by the resistance of the gas and is directed opposite to the shaft orbit.

$SR = \Omega/\omega$ (Fig.4c) The angular velocity of the gas volume *V* is exactly equal to that of the shaft vibration orbit. Within the limits of the approximated model here considered, there is no exchange of energy between the gas and the shaft, therefore the seal is neither stabilizing nor destabilizing. The cross-coupled stiffness is zero.

$SR > \Omega/\omega$ (Fig.4d) The angular velocity of the gas volume *V* is higher than the angular velocity Ω of the shaft orbit. In this situation the gas transfers part of its kinetic energy to the vibrational motion of the rotor and therefore has a destabilizing effect. If the shaft moves along the *x* axis, thus reducing the seal clearance in that direction, it is pushed (accelerated) in the same direction *y* of its orbit by the gas *V* impinging on it. This is represented by cross-coupled terms *k* and *c* in the stiffness and damping matrices.

The above description shows that in order to improve the rotordynamic stability of the compressor it is necessary to reduce as much as possible the swirl ratio of a labyrinth seal. It should be observed that in most rotating machines the main component of the radial vibration is synchronous with the rotation, i.e. $\Omega=\omega$; this component is also indicated as 1X. If only the 1X vibration is addressed, the above relations show that in order to preserve rotordynamic stability it is sufficient to have SR<1, and this would require little effort, since for centrifugal compressor applications it is very uncommon to have SR≥1 in a labyrinth seal (Baumann, 1999). For normal labyrinth seals on impeller shrouds the SR is often estimated to range between 0.5 and 0.7 (API684, 2005; 3.4.2). The problem is that usually the 1st natural frequency of compressor rotors (ω_{CS1}) is significantly lower than their rotating speed: the ratio CS1/MCS is typically lower than 0.6 and may be as low as 0.3 or 0.4. Since many sources of excitation may cause a vibration response of the rotor at its natural frequencies, the seal should be able to provide stabilizing effect not only for $\Omega = \omega_{MCS}$, but also for $\Omega = \omega_{CS1}$. Therefore the use of swirl brakes should aim to reduce SR below $\omega_{CS1}/\omega_{MCS}$.

SWIRL BRAKE OPERATION AND GEOMETRY OPTIMIZATION

Baseline analysis

To understand how the swirl brake geometry influences its performance, a Design of Experiments study (DoE) (Montgomery, 1991) was carried out. The first step consisted in the identification of a baseline design, representative of a typical real case. For this task, all the impeller seals with swirl brakes installed in the author's company compressor fleet were used to calculate the average size and geometry of the reference labyrinth seal and the swirl brake vane.

A CFD analysis of the baseline seal with and without swirl brakes implementation was carried out. Actual operating conditions (pressure, speed, and clearances) were considered for the calculations. The geometry of the vane is reproduced in Figure 5; the boundary conditions were modeled according to internal standard rules.

The preswirl at the inlet section was derived by the knowledge of the flow parameters at the impeller exit (in particular the tangential velocity of the gas, which is related to the work coefficient of the impeller). The approach to CFD analysis of swirl brakes is derived from existing literature (Nielsen et al., 1998 and 1999; Da Soghe et al., 2013). All CFD analyses have been performed using the commercial 3D Navier-Stokes solver Ansys® CFX v.14.

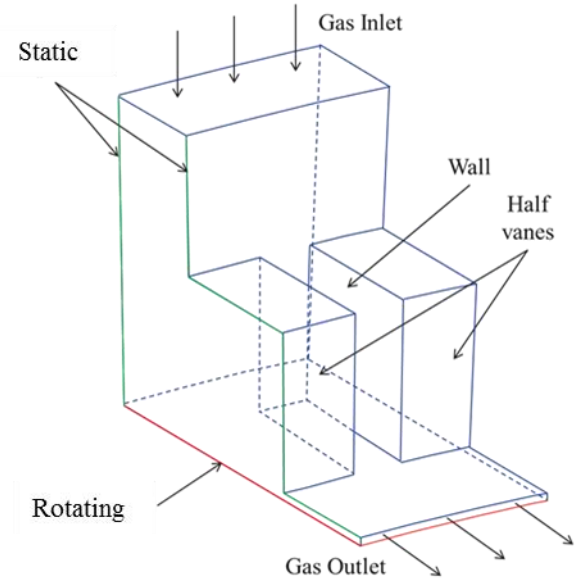

Figure 5. Swirl brake gas volume considered for CFD analysis, representing two half vanes. In green the stator surfaces, in red the rotor surface.

Below are summarized some of the most significant outcomes of the CFD analysis, that were used as a basis for developing the DoE. They are qualitatively in line with the previous studies referred above, although some difference is present in the identification of the optimum geometry.

The meridional section of the gas volume marked in red in Figure 6 is used to show the CFD results in Figures 7-9-10-11.

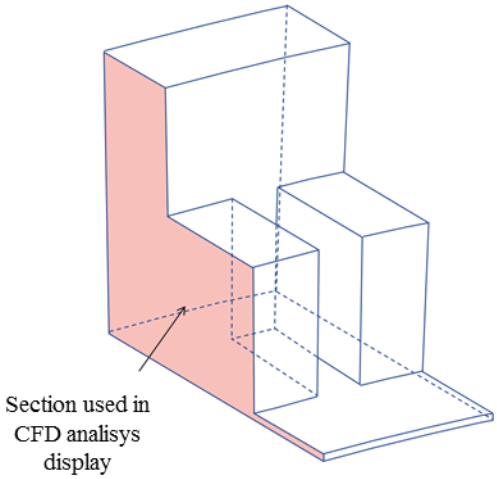

Figure 6. Gas volume referred to two half vanes. In light red the section considered for CFD output plots.

- As shown in Fig.7, the seal without swirl brakes has a mainly constant distribution of preswirl in front of the seal (red area) while the use of swirl breaks vanes introduces a gradient of preswirl inside the vane (swirl change from high value in red to smaller value in blue).
- The origin of the preswirl gradient is related to vortices that promote a local counter-rotation of the flow, thus leading to a reduction of the (average) swirl of the gas leakage flow.

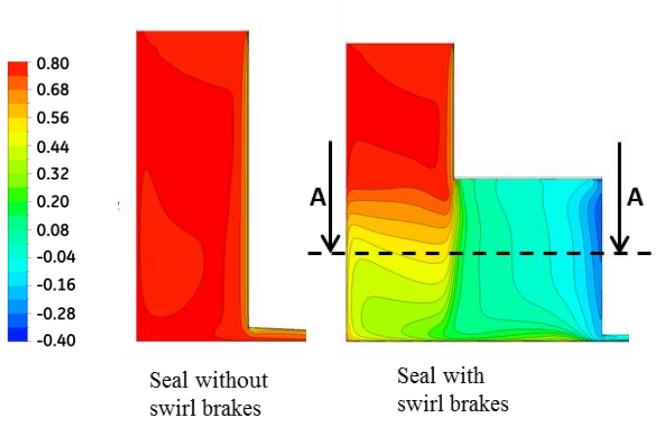

Figure 7. Contours of preswirl value (scalar), with and without swirl brakes, for a seal with and without swirl brakes. The orthogonal section A-A is the one referred in Figure 8.

- Figure 8 shows an orthogonal view of the vane, highlighting the vortex creation. The arrows represent the local direction of gas velocity, while the color represents its scalar magnitude. The velocity of the main stream of the gas approaching the vane (in yellow) is almost completely tangential, while inside the vane the flow field consists in a single large vortex.
  The alteration of the flow field caused by the swirl brakes reduces the average tangential velocity of the flowing through the seal (right end of sections in Figure 7).

Figures 7 and 8 show that the main dimensions of the vane (radial height H, circumferential pitch γ, axial length or chord A) are directly related to the flow distribution inside the vane and therefore may influence the effectiveness of the swirl brakes in reducing the preswirl of the gas.

Figure 8b shows the distribution of swirl at volume exit, downstream of the swirl brakes, that is remarkably not uniform. The swirl below the vanes reaches zero (purely axial flow) and even slightly negative values, since in that point the tangential velocity is effectively reduced by the vortices, while below the walls the gas flow has little interaction with the vanes and therefore its swirl remains relatively high. The actual preswirl value associated to the seal is the average across the whole passage area in Figure 8b.

A DoE analysis was performed, assessing the effects of vane geometry on preswirl. The variation of chord (A), height (H) and pitch (γ) was evaluated separately. The cases 2-7 listed in Table 1 were analyzed by CFD, and compared to the results obtained for case 1 (baseline). The impact of other possible geometry variations, such as the leaning of the swirl brake walls around the seal axis and/or radius, is known to be comparatively smaller (Da Soghe et al., 2013) and therefore is not addressed in the present analysis.

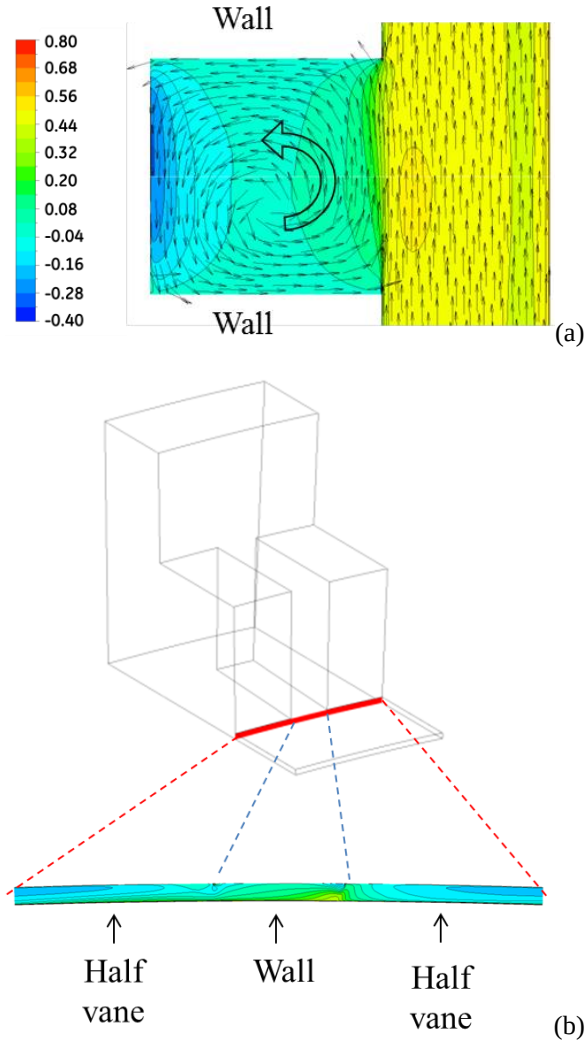

Figure 8. (a) Top view (section A-A in Fig.7, halfway along the vane radial height), showing gas velocity inside the swirl brake. The vortex formation inside the vane is clearly visible. (b) Distribution of swirl at the volume outlet.

Figures 7 and 8 show that the main dimensions of the vane (radial height *H*, circumferential pitch γ, axial length or chord *A*) are directly related to the flow distribution inside the vane and therefore may influence the effectiveness of the swirl brakes in reducing the preswirl of the gas.

Figure 8b shows the distribution of swirl at the seal inlet or exit plane from the swirl brake. The swirl is not uniform; below the vanes it reaches zero (pure axial flow) or even slightly negative values. At this location, the tangential velocity is effectively reduced by the vortices. On the other hand, below the walls, the gas flow has little interaction with the vanes and therefore its swirl remains relatively high. The seal inlet preswirl magnitude is an average across the whole passage area depicted in Figure 8b.

A DoE analysis was performed, assessing the effects of vane geometry on preswirl. The variation of chord (*A*), height (*H*) and pitch (γ) was evaluated separately. The cases 2-7 listed in Table 1 were analyzed by CFD, and compared to the results obtained for case 1 (baseline). The impact of other possible geometry variations, such as the leaning of the swirl brake walls around the seal axis and/or radius, is known to be comparatively smaller (Da Soghe et al., 2013) and therefore is not addressed in the present analysis.

Design ID	Geometry
1	Baseline geometry
2	Vane chord (*A*) + 50%
3	Vane chord (*A*) - 50%
4	Vane height (*H*) + 50%
5	Vane height (*H*) - 50%
6	Vane pitch (γ) + 50%
7	Vane pitch (γ) - 50%

Table 1. List of geometric parameters varied in DoE analysis

Variation of vane chord (A)

As shown in Figure 9 the reduction or extension by 50% of the vane chord (*A*) does not alter qualitatively the velocity distribution within the vane. Even at minimum vane chord, the vane dimension is enough to create a vortex and therefore to significantly reduce the gas swirl, even if the efficiency of the swirl brake is slightly reduced in case of shorter chord (see Figure 12a).

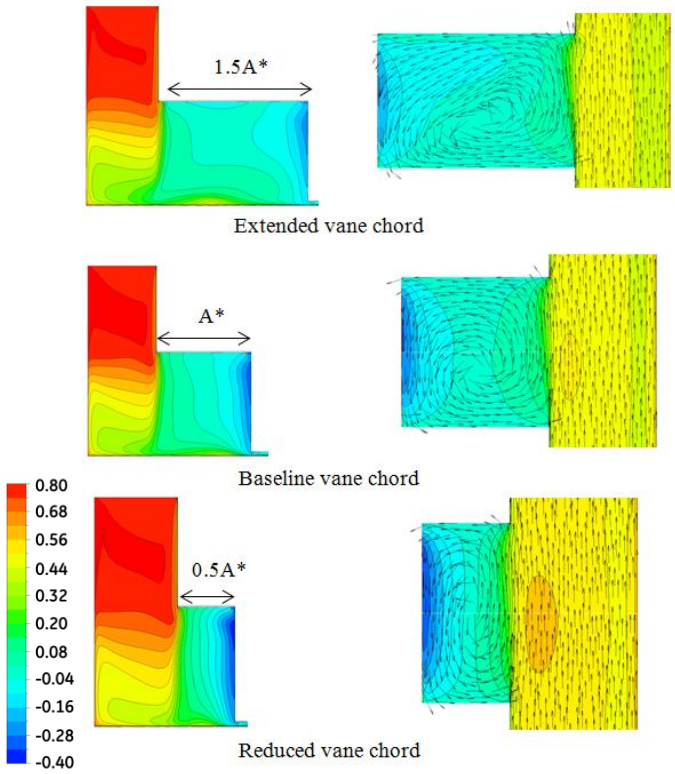

Figure 9. Effect of variation of vane chord on swirl ratio (left) and velocity distribution (right).

Variation of vane height (H)

The same analysis was carried out for variations of the vane height (*H*). Figures 10 shows the local preswirl distribution inside vanes of different height. Preswirl is qualitatively very similar for the Baseline and Extended cases,

while in the Reduced case some difference is visible: the contour lines between SR=0 and SR=0.5 are concentrated in a small L-shaped area corresponding to the edge of the wall, while for the other two cases they are smeared on a larger area. This means that in the Reduced case the tangential velocity of the flow is not reduced gradually in the annular cavity, but only during its flow across the vanes. Even if the overall swirl brake performance is in line with the other cases (Figure 12b), the swirl brake is approaching a limit: for a further reduction of *H* the situation would become similar to the no-swirl brake case of Figure 7, with the high-SR flow (red color) shifting towards the seal clearance at the right end of the section.

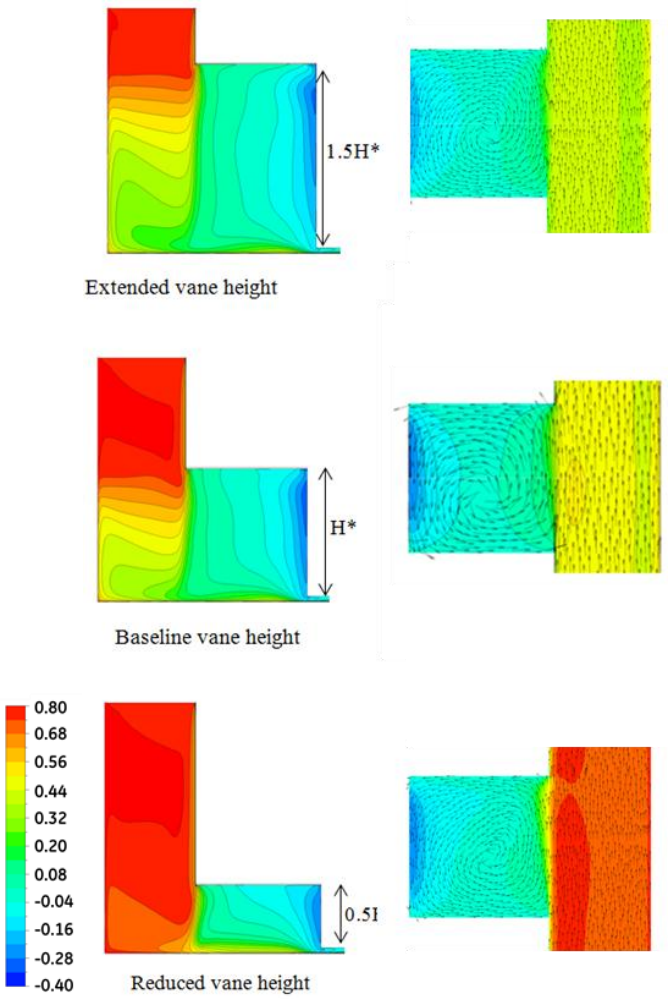

Figure 10. Effect of vane height (H) variation on swirl ratio.

Variation of vane pitch (γ)

Figure 11 shows the velocity distribution (arrows) and scalar magnitude (color scale) for the analyzed pitch values. In analogy to what observed for *A* and *H*, varying γ by ±50% has a relatively small effect on the preswirl value, as shown in Figure 12c. In particular the preswirl is higher for lower γ; this could appear counter-intuitive since in a seal equipped with more vanes the straightening effect is expeceted to be stronger (lower volume/area ratio of the vanes, thus higher friction between gas and stator surfaces). The reason is due to another effect, related to the ratio γ/t between vane pitch and wall thickness: an increase of the number of vanes corresponds to a reduction of γ/t (since there is a lower limit for *t*, due to structural reasons). This means that a higher percentage of the gas leakage flows directly to the seal passing below the wall, without entering a vane and therefore maintaining its tangential velocity unaltered. This decreases the overall efficiency if the swirl brakes in reducing preswirl.

For the reduced vane, the velocity distribution shows a steep change at the interface between the annular cavity and the vane. As described in the previous paragraph for the variation of vane height, this means that the reduced vane case is approaching a limit condition; if γ is further reduced, the situation becomes similar to the no-swirl brake case of Figure 7, with sudden loss of efficiency in reducing preswirl.

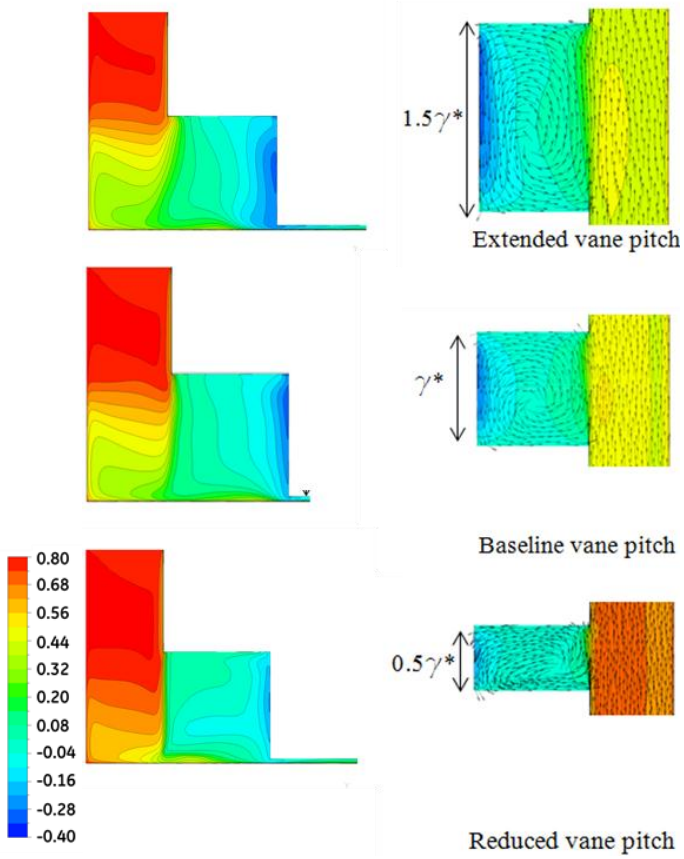

Figure 11. Effect of variation of vane pitch (γ) on gas velocity distribution.

Basing on these results the swirl brakes design philosophy has been improved considering the optimum combination of the three parameters showed above. As shown in Figure 12, the most significant result is anyway the low sensitivity of the swirl brake efficiency (defined as its capability to reduce the preswirl of the gas leakage) to the vane geometry in a reasonable range within the baseline.

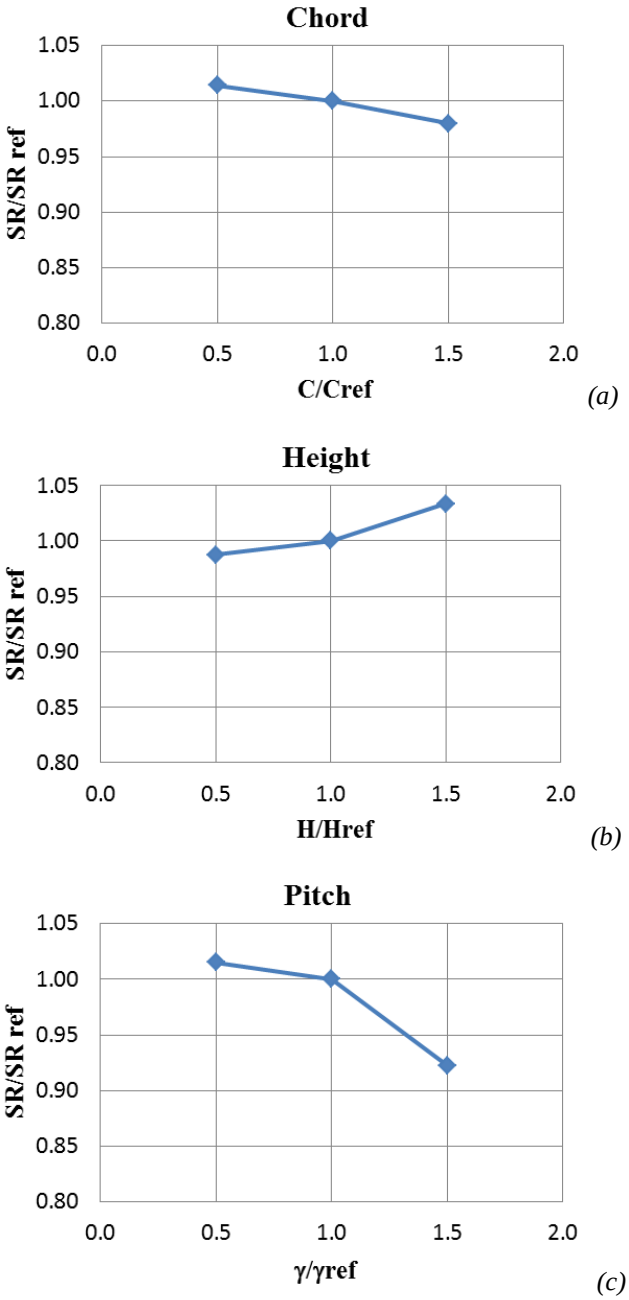

Figure 12. Preswirl variation with chord (a), height (b) and pitch (c). On the vertical axis the preswirl values are normalized with the value obtained for the baseline case.

MODEL VALIDATION

Measurement of Logarithmic Decrement

Stability tests are performed routinely by OEMs to verify the rotordynamic behavior of compressors. Usually a magnetic exciter (ME) is installed at the shaft end (opposite to the coupling) to apply a periodic load excitation to the rotor, and the induced rotor vibration is recorded at the bearing sensors. The periodic excitation is generally applied with variable frequency ("frequency sweep") to measure the response of the system over the frequency range of interest. An order tracking analysis of vibration signals returns a set of Frequency Response Functions (FRFs), and using several curve fitting techniques the natural frequencies and damping properties of the compressor are identified. The main disadvantage of a traditional stability test is the requirement of a dedicated test set up to install the ME, with impact on the rotor and stator part of the centrifugal compressor and on the control system.

As an alternative to the traditional test requiring an external additional force to be applied on the rotor, a method named Operational Modal Analysis (OMA) can be applied, consisting in the identification of modal parameters through vibration data analysis. This paragraph provides some basic information on what is OMA and how it is applied to the measurement of log.dec. on rotating machines. A detailed theoretical treatise of this analytical method is presented in (Zhang et al., 2005), while its application to the measurement of log.dec. on centrifugal compressors is described in detail in (Guglielmo et al., 2014).

OMA is a technique for modal parameter estimation that does not require the knowledge of the input loading force. In OMA some or all the excitation forces applied to the structure are unknown. If for those input forces a Gaussian white noise distribution is assumed, containing the same energy level at all frequencies, then the output spectrum is fully representative of the structure information and all modes inside the range are equally excited. Unfortunately, this assumption is not correct for a real operating centrifugal compressor rotor, as there is always input at some frequencies that contains more energy than others. Hence the unknown excitation forces are assumed to be the result of a "shaping" of the white noise by an excitation mechanism; acting like a linear filter on the flat white noise and transforming it into the real energy distribution applied to the rotor (see Fig.13).

The basic idea behind OMA is that the observed response is the natural vibration of a combined system, obtained by the interaction between the structure under test and the excitation mechanism. Physical modes related to structure and excitation are identified all together, and subsequently their frequency content and spatial properties allows the user to separate them.

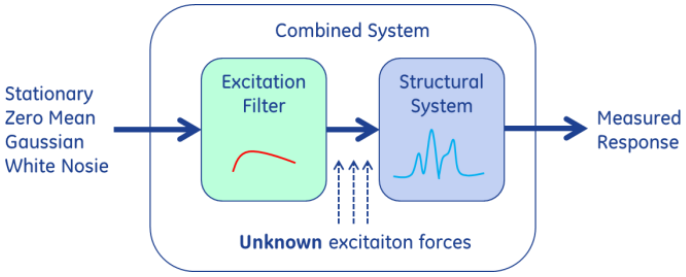

Figure 13. Schematic representation of OMA model

During the performance test of a centrifugal compressor, vibration signals are recorded under steady state operating conditions to perform the operational modal analysis of the rotor. According to the definition of the spatial position of four vibration sensors in the machine a test model of rotor is created, here reported in Fig.14, and it is used to visualize the vibration shape of the identified mode.

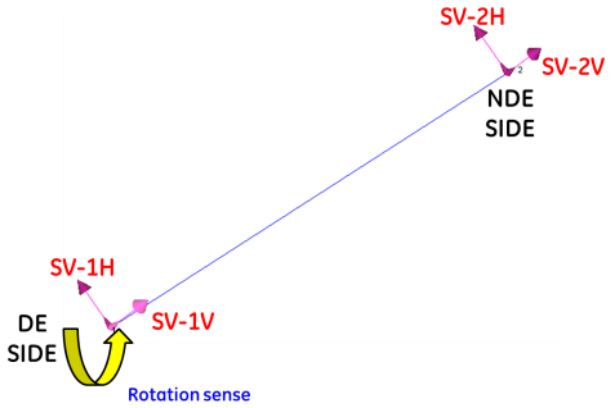

Figure 14. Schematic geometry used for applying OMA to rotor radial vibrations.Tags in red refer to the vibration sensors (1 and 2 are the two journal bearings, H and V are orthogonal directions of measurement).

A set of several auto-power frequency spectra, $G_{ii}(\omega)$, and cross-power frequency spectra, $G_{ij}(\omega)$, is calculated on the recorded vibration signals. Spectra are then averaged in order to reduce noise. At the end of the average process an output matrix $[G(\omega)]$ of the structure is created, representing the statistical response of structure under steady state conditions.

$$[G\ (\omega)] = \begin{bmatrix} G_{i,i}(\omega) & \cdots & G_{i,j}(\omega) \\ \vdots & \ddots & \vdots \\ G_{j,i}(\omega) & \cdots & G_{j,j}(\omega) \end{bmatrix} \qquad (11)$$

The use of $G_{ii}(\omega)$ and $G_{ij}(\omega)$ functions is typical in the analysis of random vibrations where each signal is analyzed in term of its statistical properties during the acquisition time.

In analogy to the modal decomposition theory (Hailen et al., 2004), singular value decomposition (SVD) factorization is applied to the output matrix $[G(\omega)]$ and the resulting singular values are plotted over the frequency axis. At a given frequency, the number of positive (non-zero) singular values corresponds to the number of modes that are contributing to the overall vibration of the structure.

The output matrix [G(ω)] is converted from the frequency domain (ω) to the time domain (τ) and the corresponding correlation functions, $G_{i,i}(\tau)$ and $G_{i,j}(\tau)$, are used to identify the properties of the structure by means of a dedicated model (Brinker and Andersen, 2006) denoted as Stochastic (SSI), that is a "black-box" multiple degree of freedom algorithm that fits the response of a generic structure with a linear equations system, yielding a global estimation of its modal parameters. It allows not only to identify the frequency and damping of the identified vibration modes, but also to determine the associated mode shape.

The use of OMA for logarithmic decrement evaluation on centrifugal compressors was validated at the authors' Company through a direct comparison with a traditional stability test employing a magnetic exciter, confirming the reliability of its results (Guglielmo et al., 2014). The broad-band excitation source applied to the rotor is represented by the aerodynamic force of the inlet gas flowing into the compressor suction. This force in a high pressure centrifugal compressor tested at full load conditions is large enough for the purpose of the analysis.

Case Study

In order to validate the calculation model described in the present paper, the full load test of a high pressure centrifugal compressor was considered. The operating data are summarized in Table 2. The compressor is composed by a single section with 5 stages in line; each labyrinth seal on impeller eye is equipped with swirl brakes, while on the balancing drum there is a labyrinth seal with shunt holes device. It was purposely avoided to select a compressor equipped with honeycomb seal, since the large aerodynamic effects related to this seal type (and the associated uncertainties of calculation models) would make more difficult the assessment of swirl brake effects.

An extensive data acquisition was performed during the tests and the most coherent data (i.e. the least affected by measurement noise, thus yielding the most reliable output) have been selected for OMA application. The rotordynamic model included a detailed geometrical description of the rotor and the journal bearings, and was able to correctly predict the frequency and amplification factor of the 1st critical speed under no load conditions (mechanical running test performed under vacuum).

Compressor Type	In-line, 5 stages
Inlet pressure [bar-a]	80
Outlet pressure [bar-a]	131
Inlet mass flow [kg/s]	146
Rotational speed [rpm] [Hz]	6512 108.5
Absorbed Power [kW]	8035

Table 2. Compressor operating parameters during first run

Data acquired during this run was post processed with the OMA method. The SVD of the response matrix allowed to identify two excited modes between 78.3 and 92.07 Hz (see Fig.15), presumably corresponding to the forward and backward modes associated to the 1st critical speed. The process algorithm is able to recognize and discard the peaks due to signal noise, basing on the values of several parameters (damping, frequency deviation etc.) largely different from those of actual vibration modes. Modes are well separated and they are present also at the lowest order of mathematical model. The associated vibration shapes show a MAC (Modal Assurance Criterion) (Ewins, 1984) close to 0.07, that means the identified modes are orthogonal and they travel in the backward and forward directions, respectively, when compared to the shaft sense of rotation (see Figure 16).

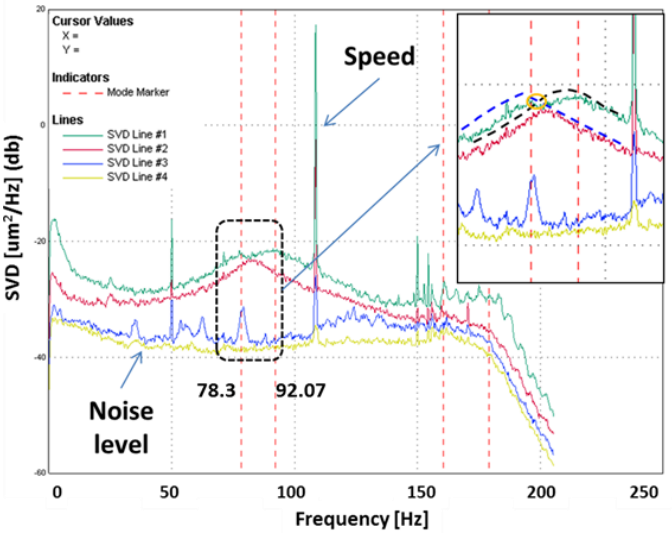

Figure 15. OMA output plot.The curves represent the SVD output of the matrix [G(ω)], derived by radial vibration measurements. The dashed lines identify the peaks corresponding to natural frequencies of the rotor.

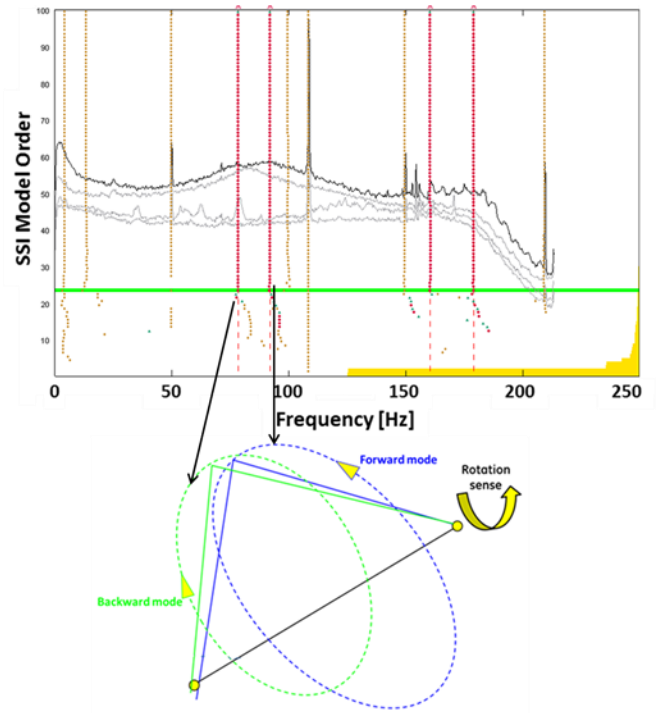

Figure 16. Stabilization diagram of model identification with SSI (Stochastic Subspace Identification) algorithm.

To quantify the preswirl value at the impeller eye seals that leads the rotordynamic model to match the measured log. dec., a set of calculations was performed with this preswirl varying between 0 and 0.5. Two limit cases were considered for the preswirl on the balance drum seal, that is equipped with radial shunt holes: SR=0.0, corresponding to ideal shunt holes operation (all the leakage flowing through the seal comes from the shunt holes, therefore the tangential component of gas velocity is zero) and SR=0.2, that according to authors' experience is a conservative estimation of the possible deviation from an ideal case (some residual tangential component of the average gas velocity at seal inlet is present).

Table 3 shows the predicted values of frequency and log.dec. for the first forward natural frequency of the rotor; according to this study, the best matching with experimental data is obtained by imposing SR between 0.1 and 0.3 for the labyrinth seals equipped with swirl brakes. This is also in good agreement with the results of CFD analysis, and is not far from some SR values suggested in literature, usually ranging between 0 and 0.25 (e.g. Camatti et al., 2006; Baumann, 1999; API684, 2005). The slight frequency offset (1st forward frequency detected by OMA at 78.3Hz) possibly suggests some underestimation of the direct stiffness associated to the labyrinth seals on impellers and/or the balance drum.

Preswirl @ impeller eye seals	Preswirl @ Bal. Drum seal = 0.0		Preswirl @ Bal. Drum seal = 0.2	
	Log. Dec.	1st FWD Freq. [Hz]	Log. Dec.	1st FWD Freq. [Hz]
0.5	0.87	87.77	0.82	87.62
0.4	0.92	87.93	0.87	87.77
0.3	0.97	88.13	0.92	87.96
0.2	1.02	88.37	0.97	88.19
0.1	1.07	88.65	1.02	88.45
0.0	1.11	88.96	1.06	88.75

Table 3. Frequency and log.dec. of 1st forward vibration mode, calculated for different values of Swirl Ratio at seal inlet.

CONCLUSIONS

The present study addressed the rotordynamic effect of swirl brakes on labyrinth seals, focusing on two aspects:

- *Geometry optimization*: analyzing the relation between the dimensions of the swirl brake vane and the efficiency in reducing the swirl ratio of the gas.
- *Swirl Ratio (SR) measurement*: measuring the log.dec. of a compressor equipped with swirl brakes on impeller labyrinth seals, and matching it with rotordynamic calculations to derive the actual swirl ratio obtained at those seals.

Regarding the optimization of swirl brake geometry, the results of the present study highlight a low sensitivity of swirl brake performance to variations in the size of the cell, within the considered variation range (+/- 50% from the values of the baseline swirl brake vane). CFD results show that even if the shape of the vane undergoes significant variations, the velocity distribution is qualitatively unchanged: inside the vane a vortex forms around the radial direction, neutralizing almost completely the tangential velocity component at seal inlet. This conclusion is welcome from the standpoint of compressor design and manufacturing, suggesting that the swirl brake vane shall not necessarily be redesigned for each project basing on

the specific compressor stage geometry and operating parameters. It is possible to define a standard vane geometry (pitch, height and chord resulting in the lowest swirl ratio of the leakage, according to CFD output), and just scale all the dimensions with the diameter of the seal where the swirl brakes shall be applied. This simplified design process may result in a significant reduction of design and manufacturing costs.

A case study of an actual compressor served to get some experimental confirmation of the outcome of CFD analysis, about the swirl ratio associated to seals with swirl brakes. The frequency and log. dec. of the first forward natural frequency of the rotor is directly influenced by the SR in the impeller seals; therefore, using a rotordynamic model already verified in no-load conditions, the SR value can be derived as the one that allows a best fitting between calculation and test results. For the analyzed centrifugal compressor, this activity returns a SR value between 0.1 and 0.3. The analysis of additional experimental data coming from other high pressure compressor tests is ongoing and will allow to further refine this value. In the meanwhile for all rotordynamic calculation purposes it appears conservative to consider 0.3 as seal SR in presence of swirl brakes.

NOMENCLATURE

CSn	n^{th} rotor critical speed
DoE	Design of Engineering
FFT	Fast Fourier Transform
MAC	Modal Assurance Criterion
MCS	Maximum Continuous Speed
ME	Magnetic Exciter
OMA	Operational Modal Analysis; occasionally also referred to as Output-only Modal Analysis
SR	Swirl Ratio, or preswirl
SSI	Stochastic Subspace Identification
SVD	Singular Value Decomposition
1X	Synchronous vibration

A	Swirl brake vane axial length (chord] [mm]
c	Damping coefficient, cross-coupled [Ns/m]
C	Damping coefficient, direct [Ns/m]
D	Shaft diameter [mm]
F	Force [N]
G	Frequency spectrum, function of ω.
h	Seal radial clearance [mm]
H	Swirl brake vane radial height [mm]
k	Stiffness coefficient, cross-coupled [N/m]
K	Stiffness coefficient, direct [N/m]
r	Radial displacement [mm]
R	Shaft radius [mm]
v	Gas velocity [m/s]
V	Gas volume [m3]
x	Horizontal direction
y	Vertical direction
γ	Swirl brake vane pitch [°]
ω	Shaft angular velocity of rotation [rad/s]
Ω	Shaft angular velocity of precession [rad/s]

REFERENCES

API 617, 2002, "Axial and Centrifugal Compressors and Expander-Compressors for Petroleum, Chemical and Gas Industry Services", Seventh Edition, American Petroleum Institute, Washington, D.C.

API 684, 2005, "API Standard Paragraphs Rotordynamic Tutorial: Lateral Critical Speeds, Unbalance Response, Stability, Train Torsionals, and Rotor Balancing", Second Edition, American Petroleum Institute, Washington, D.C.

Baumann, U., 1999, "Rotordynamic Stability Tests on High-Pressure Radial Compressors" *Proceedings of the 28th Turbomachinery Symposium*, Turbomachinery Laboratory, Texas A&M University College Station, Texas, pp. 115-122.

Brinker, R. and Andersen, P., 2006, "Understanding stochastic subspace identification", Proceedings of the 24th International Modal Analysis Conference (IMAC-XXIV), St. Louis, Missouri.

Camatti, M., Moore, J. J., Smalley, A. J., Vannini, G. and Vermin, L., 2006 , "Investigation of a Rotordynamic Instability in a High Pressure Centrifugal Compressor due to Damper Seal Clearance Divergence", *7th IFToMM Conference on Rotor Dynamics*, Vienna, Austria.

Childs, D. W., 1993, "Turbomachinery Rotordynamics", John Wiley & Sons, New York, New York, p.345.

Da Soghe, R., Micio, M., Andreini, A., Facchini, B., Innocenti, L. and Ceccherini, A., 2013, "Numerical Characterization of Swirl Brakes for High Pressure Centrifugal Compressors", *ASME Turbo Expo 2013*, San Antonio, Texas, Paper No. GT2013-94075, pp. V06CT40A001.

Ewins, D.J., 1984, "Modal Testing: Theory and Practice", John Wiley & Sons, Inc., New York, New York.

Guglielmo, A., Mitaritonna, N., Libraschi, M. and Catanzaro, M., 2014, "Full Load Stability Test on LNG Compressor", *ASME Turbo Expo 2014*, Dusseldorf, Germany, ref. GT2014-25353.

Iwatsubo, T., and Iwasaki, Y., 2002. "Experimental and Theoretical Study on Swirl Braked Labyrinth Seal", *Proceedings of the 6th International Conference on Rotor Dynamics*, Sydney, Australia, pp. 564-571.

Montgomery, D.C., 1991, "Design and Analysis of Experiments", John Wiley & Sons, New York.

Moore, J. and Hill, D., 2000, "Design of Swirl Brake for High Pressure Centrifugal Compressors using CFD Techniques", *International Symposium on Transport Phenomena and Dynamics of Rotating Machinery*, Honolulu, Hawaii.

Muszynska, A., 2005, “Rotordynamics”, CRC Press, Boca Raton, Florida.

Nielsen, K., Myllerup, C. M., and Van den Braembussche, R. A., 1999, “Parametric Study of the Flow in Swirl Brakes by Means of a 3D Navier-Stokes Solver”, *Transactions of the Third European Conference on Turbomachinery*, London, UK, pp. 489-498.

Nielsen, K., Van den Braembussche, R. A. and Myllerup, C. M., 1998, “Optimization of Swirl Brakes by Means of a 3D Navier-Stokes Solver”, *ASME Technical Paper*, Vol. 98-GT-32B.

Zhang, L., Brincker, R. and Andersen, P., 2005, “An Overview of Operational Modal Analysis: Major Development and Issues”, *Proceedings of the 1st International Operational Modal Analysis Conference*, Copenhagen, Denmark, pp. 179–190.

ACKNOWLEDGEMENTS

The Authors thank Mr. Riccardo Da Soghe for his contribution to the present work, by means of the extensive CFD campaign that he carried out and of the insightful interpretation of the results provided.